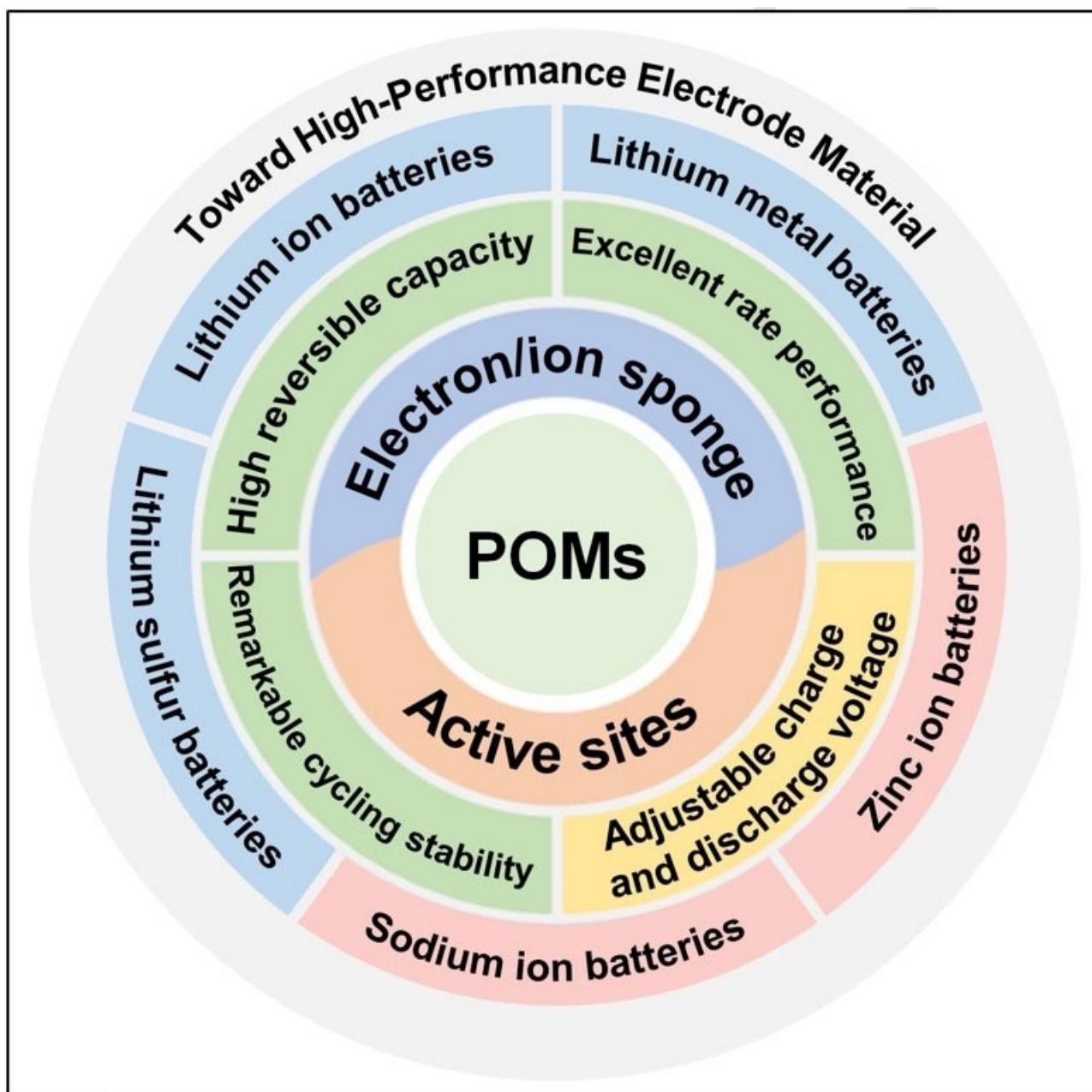


Polyoxometalates (POMs) with Ion/Electron-Sponge Properties and Abundant Active Sites as Emerging Electrode Materials for Secondary Batteries: A Review

Jinkun Wang,^[a] Li Wang,^[a] Yang Yang,^[a] Hong Xu,^[a] and Xiangming He^{*[a]}



Faced with the increasingly severe energy and environment issues, eco-friendly and efficient energy storage/transformation technology has become a research hotspot. Due to the ion/electron-sponge properties and superior catalytic performance, polyoxometalates (POMs) have broad prospects in improving the performance of electrodes and batteries. In this paper, the structural characteristics and physical/chemical properties of POMs are introduced, and the recent research progresses of

POM-electrodes for various battery systems are reviewed. By analyzing the relationship between the composition, structure and electrochemical performance of POMs, the advantages and challenges of applying POMs as electrode materials are explained, and the practical modification strategies for improving the performance of POM-electrode are proposed, aiming to provide reference for the further investigation and application of POMs in energy storage field.

1. Introduction

Polyoxometalates (POMs) refer to a class of inorganic materials, which are usually produced by the condensation of one or more oxygenated salts with simple structures under certain conditions.^[1] The history of POMs goes back to the discovery of heteropoly acids in the late 18th century.^[1a] In 1826, Berzelius reported the synthesis of heteropoly acid $(\text{NH}_4)_3\text{PMo}_{12}\text{O}_{40} \cdot \text{H}_2\text{O}$ for the first time.^[2] Compared with simple acids, POMs with multicore structure have more diverse properties (such as catalysis, magnetism, redox properties, photochemical activity, etc.) and have attracted extensive attention in many fields including catalysis and energy storage.^[1b,c] Investigations on POM-electrode date back to the late 20th century. In 1997, Gómez-Romero P and Lira-Cantú M reported the typical POM anion, $[\text{PMo}_{12}\text{O}_{40}]^{3-}$ (PMo_{12}), and analyzed the properties, electrochemical applications, as well as prospects, of hybrid materials containing POMs.^[3] Under the trend of energy saving and emission reduction, rechargeable batteries are in great demand, and people have increasingly high requirements on the capacity, cost, safety and stability of batteries.^[4] POMs have showed great potential in improving battery performance with their unique properties and have attracted the interest of many researchers.^[5] The progress timeline of research on POM-electrodes for secondary batteries is shown in Figure 1.

In the past decade, the research on application of POMs in various battery systems has gradually increased (Figure 2a and b). Compared with the application of POMs in electrolyte and separator, the application of POMs in battery electrodes has attracted more attention (see in Figure 2c). As an emerging electrode material, POMs can not only act as "ion sponges" which can reversibly absorb and release the ions that transfer charge (such as Li^+ , Na^+ , and Zn^{2+}), but play the role of "electron sponges" to promote the kinetics of electrode reactions.^[1a,6] Therefore, many studies have tried to apply POMs into secondary batteries including lithium-ion batteries (LIBs), lithium-metal batteries (LMBs), sodium-ion batteries (SIBs), and zinc-ion batteries (ZIBs). Besides, the transition metal atoms whose oxidation and reduction are reversible in POMs can act as active sites to catalyze the conversion of active materials in

batteries.^[7] Hence, POMs are able to be applied in lithium-sulfur batteries (LSBs) to facilitate the conversion of lithium polysulfides, thereby restraining the shuttle effect. Such batteries with POMs as the electrode materials are called molecular cluster batteries (MCBs).

In recent years, there are many valuable discoveries on the fundamentals and applications of POMs in electrode materials. In this paper, the properties of different POMs and their applications in electrode materials for a variety of battery systems are reviewed, as well as the relationship between the structure and electrochemical performance of POMs. Three modification strategies are proposed, aiming to enable the POM-electrodes to better meet the practical requirements.

2. Physical and Chemical Characteristics of POMs

The general formula of the anions of POMs can be expressed as $[\text{X}_x\text{M}_m\text{O}_n]^{a-}$. The anions of POMs are generally ordered clusters composed of transition-metal-oxygen polyhedral $[\text{MO}_y]$ ($y=4-7$), in which M is usually Mo, W, V, Nb or Ta, and the transition metal atoms are connected by oxygen bridge bonds.^[5a,8] The central atom, X, of POMs can be either metallic or non-metallic, such as Mo, W, V, Nb, Ta, P, Si, B, etc., and $[\text{MO}_y]$ acts as the ligand of the central atom. If a POM obtained by dehydration and condensation of only one kind of oxysalt, the POM, in which the atom X and the atom M of $[\text{X}_x\text{M}_m\text{O}_n]^{a-}$ are the same, belongs to isopoly salts. If a POM obtained by dehydration and condensation of two or more kind of oxysalts, then the POM, in which the atom X is different with M, belongs to heteropoly salt. The POMs commonly used in battery research are generally heteropoly salts whose structure can be described as Figure 3(a). According to the number of central atoms and the arrangement of $[\text{MO}_y]$, POMs can be divided into a variety of structures. Among them, the most classic structures are the Keggin structure and Dawson structure (see Figure 3b), and most of the other complex structures are based on these two structures.^[1a] POMs in various structures can form nanomaterials of different dimensions and shapes by self-assembly, performing a variety of functions to meet different requirements.^[9]

The physical and chemical properties of POMs are obviously different from the properties of traditional transition metal oxides due to the unique structural characteristics of POMs.

[a] J. Wang, Prof. L. Wang, Prof. Y. Yang, Prof. H. Xu, Prof. X. He
Institute of Nuclear and New Energy Technology
Tsinghua University
Beijing 100084 (P. R. China)
E-mail: hexm@tsinghua.edu.cn

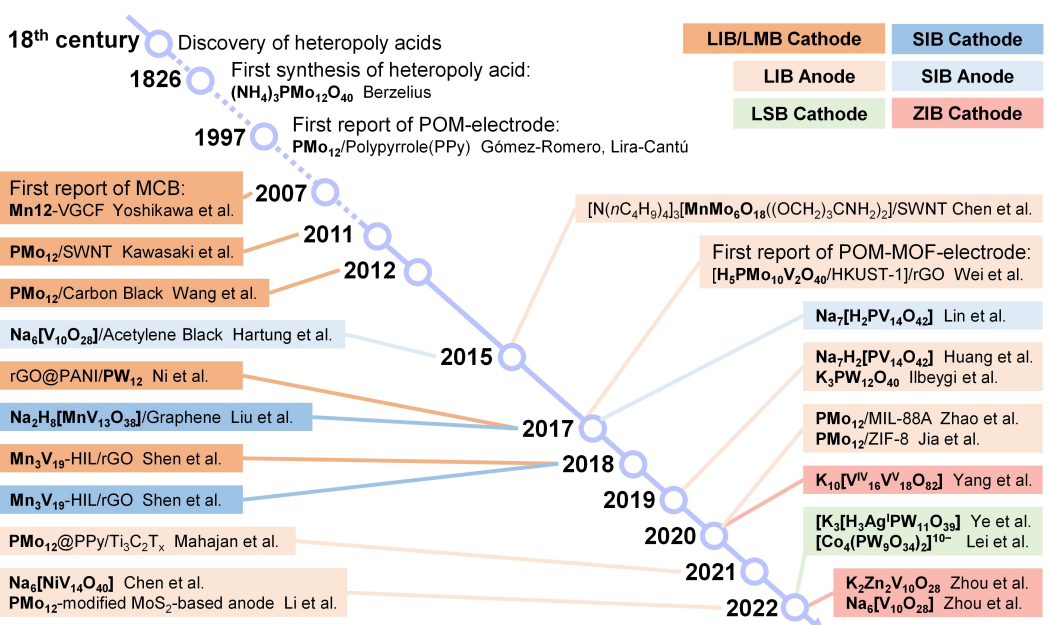


Figure 1. Historical progress of scientific research on POM-electrodes of secondary batteries. Different colors are used to represent different application scenarios.

Due to the ability to reversibly absorb and release a number of ions, POMs are figuratively called "ion sponges". As ion

sponges, POMs can be used not only to store specific ions, but also to regulate ion concentration distribution. Similarly, POMs



Jinkun Wang is currently a Ph.D. student in Tsinghua University under the supervision of Prof. Xiangming He. He received his B.Eng. degree (Materials Science and Engineering) from Tianjin University (2021). His research interest focus on electrochemical energy storage, including lithium-ion batteries and lithium metal electrodes.



Prof. Li Wang is an associate professor at Institute of Nuclear and New Energy Technology, Tsinghua University. She received Ph.D. in analytical chemistry from Tsinghua University in 2004. Her research focuses on key materials and technology for secondary batteries of high energy density and safety.



Prof. Yang Yang received her PhD degree from Tsinghua University in 2017. She joined Prof. Yen Wei's group at Department of Chemistry, Tsinghua University, as a postdoc from 2017 to 2020. Then she joined the Institute of Nuclear and New Energy Technology, Tsinghua University as an Assistant Professor in 2020. Her research focuses on the functional polymeric materials containing dynamic covalent bonds for smart materials, including liquid-crystalline elastomers for soft actuators, vitrimers, stimuli-responsive polymers, polymeric nanocomposites, and so on.



Prof. Hong Xu received his bachelor's degree in polymers at Shanghai Jiao Tong University in 2009 and his Ph.D. in structural molecular science at Institute for Molecular Science in 2015. He is currently an associate professor at Tsinghua University. His research interest lies in the fields of extreme ultraviolet photoresists, covalent organic frameworks, and lithium-ion batteries.



Prof. Xiangming He is a professor and the group leader of the Lithium-ion battery Laboratory in the Institute of Nuclear and New Energy Technology, Tsinghua University. He received his bachelor's, master's degrees and PhD from Tsinghua University. His research focuses on the design and application of functional materials for energy storage (lithium-ion batteries) and fundamental understanding of related electrochemical processes.

Batteries & Supercaps 2023, 6, e202200510 (3 of 12)

© 2023 Wiley-VCH GmbH

25669223, Downloaded from https://chemistry-europe.onlinelibrary.wiley.com/doi/10.1002/batt.202200510 by University of Ulsan, Wiley Online Library on [11/11/2025]. See the Terms and Conditions (https://onlinelibrary.wiley.com/terms-and-conditions) on Wiley Online Library for rules of use; OA articles are governed by the applicable Creative Commons License

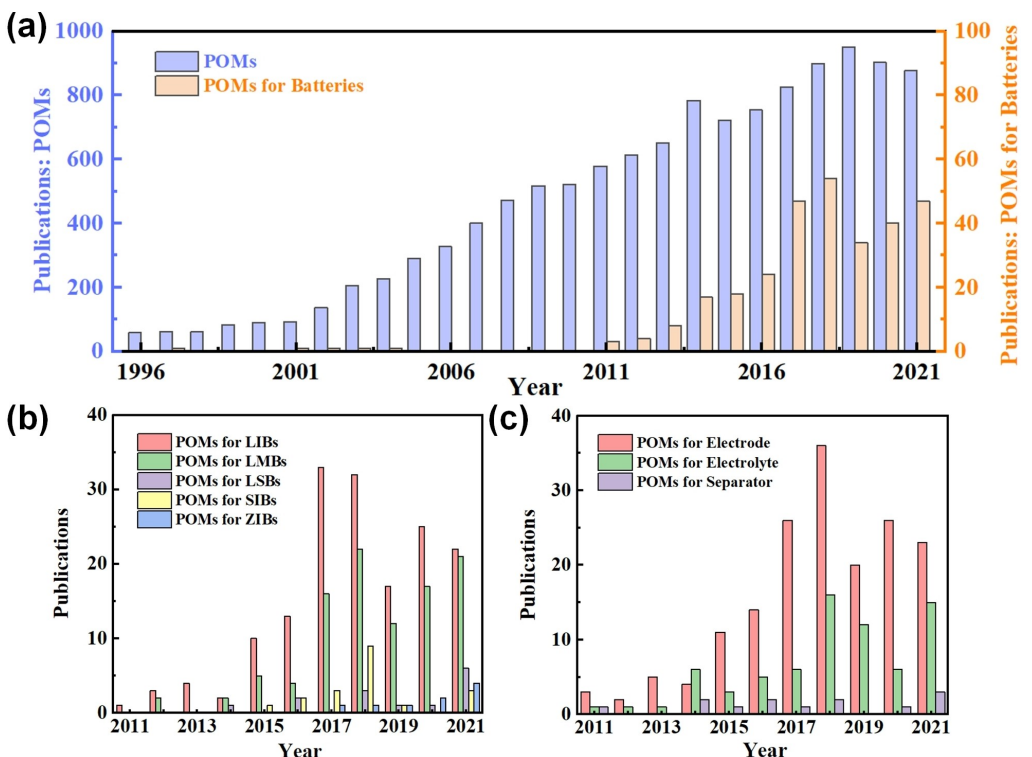


Figure 2. a) Statistics on publications of "POMs" and "POMs for Batteries" from 1996 to 2021. b) Statistics on publications about the application of POMs for different battery systems including LIBs, LMB, LSBs, SIBs, and ZIBs from 2011 to 2021. c) Statistics on publications about the application of POMs for electrode, electrolyte, and separator of batteries from 2011 to 2021. Statistics are based on the Web of Science (WOS) database.

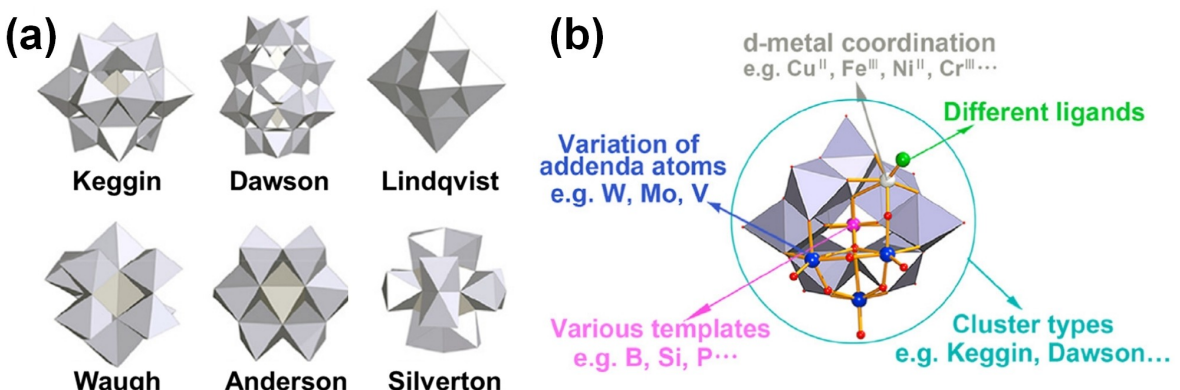


Figure 3. a) Schematic diagrams POMs in classical structures. Reproduced with permission from Ref. [12]. Copyright (2021) Elsevier. b) General rules of structure design and atomic composition of POMs. Reproduced with permission from Ref. [12]. Copyright (2021) Elsevier.

are also known as "electron sponges" because they can reversibly accept and give away electrons, switching between different electronic states.^[9] The electron-sponge property can be mainly attributed to the transition metal atoms whose valence state can reversibly change in POMs. From a thermodynamic point of view, the above two processes have low energy barriers, facilitating the occurrence of reactions and the exertion of the catalytic properties of POMs. Although the ionic conductivity of POMs is excellent, the electronic conductivity of POMs is unsatisfactory. Therefore, to meet the requirements of electrode materials, POMs need to be used in combination with matrixes with good electrical conductivity.^[3]

The electrochemical behaviors and characteristics of POMs determine the performance of corresponding POM-electrodes. The insertion/extraction of ions in POMs have similar characteristics to the solid-solution reaction rather than the phase-separation reaction. During the insertion and extraction, the content of specific ions changes continuously, and there is no obvious platform in the voltage-capacity curves of POMs. Besides, there are transition metal atoms whose valence state can reversibly change in the POMs. The exposed transition metal atoms can serve as active sites for catalytic reactions. At the same time, there are abundant external terminal O atoms acting as Lewis basic sites in the framework of POMs.^[10]

Therefore, POMs can enhance the kinetics of chemical and electrochemical reactions. In the next section, the enhanced performance of the POM-electrodes due to the unique properties of POMs is described in detail. Yang et al. reviewed the intrinsic charge carrier behaviors of POMs, as well as the relationship between the charge carrier behaviors and the cutting-edge applications of POMs.^[5a] Ueda reviewed the electrochemical properties of POMs in detail and summarized the reduction potentials of various POMs in different solutions, which can provide reference for the applications of POMs in the next generation battery system.^[11]

3. Application of POMs in Electrode Materials for Secondary Batteries

3.1. Application of POMs in electrode materials for LIBs and LMBs

As shown in Table 1, POMs can be used as cathode materials for LIBs and LMBs. Yoshikawa et al.^[13] fabricated the first rechargeable MCB. $[\text{Mn}_{12}\text{O}_{12}(\text{CH}_3\text{COO})_{16}(\text{H}_2\text{O})_4]$ was utilized as the cathode material for the battery. The MCB exhibited a large capacity ($200\text{--}250 \text{ mAh g}^{-1}$) in the first cycle. The capacity decreased significantly in the second cycle, but remained stable in following cycles. When POMs are applied to cathode materials, it is a practical strategy to combine conductive materials (such as SWNTs and rGO) with POMs whose conductivity is relatively poor. By dispersing $[\text{PMo}_{12}\text{O}_{40}]^{3-}$, a kind of Keggin-type POM, on the surface of single-wall carbon nanotubes (SWNTs), Kawasaki et al. prepared a $\text{PMo}_{12}/\text{SWNT}$ cathode as shown in Figure 4a–b.^[14] Compared with the cathode material prepared by mixing POM microcrystals with carbon fibers, the $\text{PMo}_{12}/\text{SWNT}$ cathode has superior performance due to the nanoscale dispersion of POMs which facilitates the transfer of electrons and lithium ions during the battery reactions. Wang et al. composed PMo_{12} and carbon black into the cathode material of LMBs.^[15] By measuring the fine structure of Mo K-edge X-ray absorption, they studied the reversible transition between different redox states of the POMs when being used as cathode materials. During the discharge, $[\text{PMo}_{12}\text{O}_{40}]^{3-}$ turns into $[\text{PMo}_{12}\text{O}_{40}]^{27-}$, where Mo^{6+} are reduced to Mo^{4+} , indicating that the reduction of $[\text{PMo}_{12}\text{O}_{40}]^{3-}$ is a 24-electron reaction (see in Figure 4c). The charge/discharge curves of the first two cycles of PMo_{12} are shown in Figure 4(d). The PMo_{12} cathode is almost fully charged at the beginning due to the low content of lithium in PMo_{12} , hence the 1st charging curve is very short. Shen et al. prepared composite cathode materials using POMs, ionic liquid (IL), and reduced graphene oxide (rGO).^[16] Among the cathodes they obtained, the sample $\text{Mn}_3\text{V}_{19}\text{-HIL/rGO-1}$, which is prepared with $[\text{H}_6\text{Mn}_3\text{V}_{18}\text{O}_{42}(\text{VO}_4)(\text{H}_2\text{O})_{12}] \cdot 30\text{H}_2\text{O}$ (Mn_3V_{19}) as the main active material and 1-hydroxyethyl-3-methylimidazolium chloride (HIL) as the IL, has the best cycling stability and rate performance (see Figure 4e). In Mn_3V_{19} , the 3D V-cages with Mn greatly facilitates the insertion and de-insertion of lithium ions. In

Figure 4(e), there are significant voltage plateaus at approximately 2.3–2.6 V, and this part of capacity is contributed by the redox reaction and valence change of vanadium element. Ni et al. synthesized PANI/ PW_{12} nanospheres by combining poly-aniline (PANI) with $[\text{PW}_{12}\text{O}_{40}]^{3-}$ (PW_{12}) and embedded the nanospheres into graphene sponges to fabricate 3D rGO@PANI/ PW_{12} cathode (see Figure 4f).^[17] On the one hand, the conductive polymer, PANI, facilitates electron conduction and enhances the electron storage capability of POMs. On the other hand, the 3D carbon structure not only ensures the electrical conductivity, but also improves the integrity and stability of the structure. As a result, the rGO@PANI/ PW_{12} cathode has extremely superior cycling stability in the long run.

In addition to being cathode materials for LIBs and LMBs, POMs can also be applied as anode materials for LIBs (see Table 1). Huang et al. mixed $\text{Na}_7\text{H}_2[\text{PV}_{14}\text{O}_{42}]$ (NPV), which possesses electron/ion sponge properties, with carbon black to form an anode material and applied it to LIBs.^[18] The characteristics and mechanisms of Li^+ insertion and extraction in NPV were studied in detail. The insertion and extraction of lithium ions in NPVs can be regarded as continuous processes, and the NPV electrode exhibit remarkable rate performance (see in Figure 5a and b) due to the low energy barrier of ion transfer. By analyzing the redox states of vanadium during the charge and discharge, it is found that each NPV can store at least 30 electrons, which contributes to the improvement of the energy density. Ilbeygi et al. applied $\text{K}_3\text{PW}_{12}\text{O}_{40}$ to the anode material of LIBs and investigated its lithiation mechanism by analyzing the in-situ X-ray absorption spectroscopic during cycling test.^[19] With the increase of cycling time, the anions of the $\text{K}_3\text{PW}_{12}\text{O}_{40}$, $[\text{PW}^{6+}_{12}\text{O}_{40}]^{3-}$, are gradually reduced to a completely stabilized structure, $[\text{PW}^{4+}_{12}\text{O}_{40}]^{27-}$, and the valence state of W hardly ever changes after the 10th cycle, indicating that the non-Faradaic Li^+ storage contributes most of the capacity of $\text{K}_3\text{PW}_{12}\text{O}_{40}$. Through a facile and low-cost solution process, Chen et al. synthesized $\text{Na}_6[\text{NiV}_{14}\text{O}_{40}]$ for the first time and applied $\text{Na}_6[\text{NiV}_{14}\text{O}_{40}]$ as the anode material of LIBs.^[20] The Li^+ diffusion coefficient of $\text{Na}_6[\text{NiV}_{14}\text{O}_{40}]$ is significantly higher than the Li^+ diffusion coefficients of some common anode materials including $\text{Li}_4\text{Ti}_5\text{O}_{12}$, NaVO_3 , graphite and Si. Hence, $\text{Na}_6[\text{NiV}_{14}\text{O}_{40}]$ can still exhibit superior capacity retention when charging and discharging at a higher rate. And the energy density of the full cell assembled with $\text{Na}_6[\text{NiV}_{14}\text{O}_{40}]$ as the anode and LiFePO_4 (LFP) as the cathode can reach 300 Wh kg^{-1} . SWNTs, as a good conductive material, can also contribute to the application of POMs in anode materials. Ji et al. functionalized the $[\text{MnMo}_6\text{O}_{24}]^{9-}$ with $\text{NH}_2\text{C}(\text{CH}_2\text{OH})_3$ (Tris) and obtained an organic-inorganic hybrid [$(\text{nC}_4\text{H}_9)_4\text{I}_3[\text{MnMo}_6\text{O}_{18}((\text{OCH}_2)_3\text{CNH}_2)_2]$.^[21] The hybrid molecules were attached to SWNTs to form a POM/SWNT composite material which was later applied to the anode and showed high discharge capacity, superior cycling stability and low electrochemical impedance. MoS_2 , whose theoretical capacity (670 mAh g^{-1}) is nearly twice that of graphite, is a promising anode material with a two-dimensional layered structure, but its application is limited by poor cycling performance.^[22] Li et al. modified MoS_2 -based anode with PMo_{12} which could provide

Table 1. POM-electrodes for LMBs, LIBs, SIBs, and ZIBs.

Type of POMs	Battery-electrode	Active material (Mass fraction)	Conducting material (Mass fraction)	Electrolyte	Capacity	Cycling performance	Ref.
Mn12	LMB-Cathode	Mn12 (10 wt%)	VGCF (80 wt%)	An electrolyte in EC/DEC (3:7)	200–250 mAh g ⁻¹ (1 st cycle)	Capacity: ~90 mAh g ⁻¹ after 2 cycles	[13]
PMo ₁₂	LMB-Cathode	PMo ₁₂ (10 wt%)	carbon black (50 wt%)	1 M LiPF ₆ in EC/DEC (1:1 v/v)	320 Ah kg ⁻¹ (1 st cycle)	CR: after 10 cycles: 93.8 %	[14]
PMo ₁₂	LMB-Cathode	PMo ₁₂ (10 wt%)	carbon black (70 wt%)	1 M LiPF ₆ in EC/DEC (1:1 v/v)	260 Ah kg ⁻¹ (1 st cycle)	CR: after 10 cycles: 80.8 %	[15]
Mn ₃ V ₁₉	LIB-Cathode	Mn ₃ V ₁₉ HIL/EGO (70 wt%)	Super-P (20 wt%)	1 M LiPF ₆ in EC/DMC/EMC (1:1:1, v/v/v)	210, 175, 162, 156, 152 and 121 mAh g ⁻¹ at 100, 200, 400, 1000, 2000 and 5000 mAh g ⁻¹	CR: 99.2 % after 400 cycles at 5000 mAh g ⁻¹	[16]
PW ₁₂	LIB-Cathode	rGO@PANI/PW ₁₂ (70 wt%)	Super-P (20 wt%)	1 M LiPF ₆ in EC/DEC (1:1 v/v)	285, 271, 235, 190, 160, 140 mAh g ⁻¹ at 50, 100, 200, 500, 1000, 2000 mAh g ⁻¹	CR: 72 % after 1000 cycles at 2 A g ⁻¹	[17]
KNaV ₁₀	LIB-Cathode	KNaV ₁₀ (60 wt%)	acetylene black (30 wt%)	1 M LiPF ₆ in EC/DMC (1:1 v/v)	118 mAh g ⁻¹ at 250 mAh g ⁻¹	CR: 63.9 % after 10 cycles at 50 mAh g ⁻¹	[24]
MgV ₁₀	LIB-Cathode	MgV ₁₀ (60 wt%)	acetylene black (30 wt%)	1 M LiPF ₆ in EC/DMC (1:1 v/v)	160 mAh g ⁻¹ at 250 mAh g ⁻¹	CR: 90.5 % after 60 cycles at 50 mAh g ⁻¹	[24]
NPV	LIB-Anode	NPV (70 wt%)	Super-P (20 wt%)	1 M LiPF ₆ in EC/DEC (1:1 v/v)	550, 465, 440, 410, and 365 mAh g ⁻¹ at 50, 100, 200, 500, 1000, and 2000 mAh g ⁻¹	CR: ~80 % after 150 cycles at 100 mAh g ⁻¹	[18]
K ₃ PW ₁₂ O ₄₀	LIB-Anode	mPTA (80 wt%)	1 M LiPF ₆ in EC/DEC (1:1 v/v)	1975 mAh g ⁻¹ (1 st cycle)	CR: 44.1 % after 100 cycles at 0.1 A g ⁻¹	[19]	
Na ₆ [NiV ₁₄ O ₄₀]	LIB-Anode	Na ₆ [NiV ₁₄ O ₄₀] (70 wt%)	Super P (20 wt%)	1 M LiPF ₆ in EC/DEC (1:1 v/v)	699, 538, 518, 483, 408, and 331 mAh g ⁻¹ at 100, 250, 500, 1000, 2500, and 5000 mAh g ⁻¹	CR: 110 %, 92 %, and 82 % after 400 cycles	[20]
[Mn ₅ Mo ₆ O ₂₄] ³⁻	LIB-Anode	POM/SWNT (50 wt%)	carbon black (30 wt%)	1 M LiPF ₆ in EC/DEC (1:1 v/v)	1351.3 and 654.1 mAh g ⁻¹ at 0.05 and 1 mA cm ⁻²	CR: 99.5 % after 70 cycles at 0.05 mA cm ⁻²	[21]
PMo ₁₂	LIB-Anode	Co ₅ ₂ /Mo ₅ ₂ /PDDA-rGO/PMo ₁₂ (70 wt%)	Super P (20 wt%)	1 M LiPF ₆ in EC/DEC (1:1 v/v)	722, 581, 490, and 395 mAh g ⁻¹ at 100, 200, 500 and 1000 mA g ⁻¹	Capacity: 740 mAh g ⁻¹ after 150 cycles at 0.1 A g ⁻¹ , and 5 A g ⁻¹	[22]
PMo ₁₂	LIB-Anode	PMo ₁₂ @PPy/Ti ₃ C ₂ T _x (70 wt%)	Super P (20 wt%)	1 M LiPF ₆ in EC/DMC (1:1 v/v)	327 mAh g ⁻¹ at 0.1 A g ⁻¹ (5 th cycle)	Capacity: 764 mAh g ⁻¹ after 300 cycles at 0.1 A g ⁻¹	[23]
H ₅ PMo ₁₀ V ₂ O ₄₀	LIB-Anode	[H ₅ PMo ₁₀ V ₂ O ₄₀]/HKUST-1/rGO (70 wt%)	Super P (20 wt%)	1 M LiPF ₆ in EC/DMC (1:1 v/v)	1088, 906, 846, 761, 538 and 428 mAh g ⁻¹ at 50, 100, 200, 400, 1000 and 2000 mAh g ⁻¹	CR: 99.4 % and 105.0 % after 400 cycles at 200 and 3000 mAh g ⁻¹	[25]
PMo ₁₂	LIB-Anode	PMo ₁₂ /ML-88 A (70 wt%)	acetylene black (20 wt%)	1 M LiPF ₆ in EC/DEC (1:1 v/v)	1451.60 mAh g ⁻¹ at 200 mAh g ⁻¹ (1 st cycle)	CR: 73.2 % after 100 cycles at 200 mAh g ⁻¹	[26]
PMo ₁₂	LIB-Anode	PMo ₁₂ /ZIF-8 (80 wt%)	carbon black (10 wt%)	1 M LiPF ₆ in EC/DEC (1:1 v/v)	950 mAh g ⁻¹ at 1 A g ⁻¹ (1 st cycle)	CR: 103.7 % after 200 cycles at 1 A g ⁻¹	[27]
Na ₂ H ₈ [MnV ₁₃ O ₃₈] ³⁻	SIB-Cathode	POM/G (70 wt%)	acetylene black (20 wt%)	1 M NaClO ₄ in EC/PC (1:1, v/v)	190 and 130 mAh g ⁻¹ at 0.1 C and 1 C	CR: 81 % after 100 cycles at 0.2 C	[28]
Mn ₃ V ₁₉	SIB-Cathode	Mn ₃ V ₁₉ HIL/EGO (70 wt%)	Super-P (20 wt%)	1 M NaClO ₄ in EC/PC (1:1 v/v)	194, 166, 140, 108, 89 and 73 mAh g ⁻¹ at 100, 200, 500, 1000 and 2000 mA g ⁻¹	Capacity: 92 mAh g ⁻¹ after 200 cycles at 500 mA g ⁻¹	[16]
NPV	SIB-Anode	NPV (70 wt%)	Super-P (20 wt%)	1 M NaClO ₄ in EC/PC (1:1 v/v)	318, 273, 233, 186, 135, 102, 74, and 19 mAh g ⁻¹ at 25, 50, 100, 250, 500, 750, 1000, and 2500 mA g ⁻¹	CR: 87 % after 120 cycles at 25 mA g ⁻¹	[29]
Na ₆ [V ₁₀ O ₂₈]	SIB-Anode	Na ₆ [V ₁₀ O ₂₈] (60 wt%)	acetylene black (20 wt%)	1 M NaClO ₄ in EC/PC (1:1, w/w)	276, 221, 173, and 97 mAh g ⁻¹ at 20, 50, 100, and 200 mA g ⁻¹	CR: ~48 % after 15 cycles at 50 mA g ⁻¹	[30]
KVO	ZIB-Cathode	KVO (60 wt%)	Super P (30 wt%)	2.5 M Zn(CF ₃ SO ₃) ₂ in H ₂ O	411 and 299 mAh g ⁻¹ at 0.05 and 0.5 A g ⁻¹	CR: 93 % after 4000 cycles at 3 A g ⁻¹	[31]
KZVO	ZIB-Cathode	KZVO (70 wt%)	Ketjen Black (20 wt%)	3 M Zn(CF ₃ SO ₃) ₂ in H ₂ O	225.7, 200.8, 161.2, 126.4, 100.8, and 71.1 mAh g ⁻¹ at 0.05, 0.1, 0.2, 0.5, 1, and 2 A g ⁻¹	CR: 97.6 % after 50 cycles at 0.1 A g ⁻¹	[32]
Na ₆ [V ₁₀ O ₂₈]	ZIB-Cathode	Na ₆ [V ₁₀ O ₂₈] (70 wt%)	Ketjen Black (20 wt%)	3 M Zn(CF ₃ SO ₃) ₂ in H ₂ O	279.5 mAh g ⁻¹ at 0.1 A g ⁻¹	CR: 83.8 % after 100 cycles at 0.1 A g ⁻¹	[33]

CR = capacity retention; Mn12 = [Mn₁₂(CH₃COO)₁₂]⁴⁺; PMo₁₂ = [(PMo₁₂O₄₀)₃⁷⁻]; Mn₃V₁₉ = [Mn₃V₁₉O₄₀]³⁻; Mn₃V₁₉ = [Mn₃V₁₉O₄₀]³⁻; KNaV₁₀ = [KNa₂V₁₀O₃₈]ⁿH₂O; MgV₁₀ = H₂O₂[Mg₁₀V₁₈O₄₂]²⁻; KVO = [KVO₂]²⁻[PO₄₂]³⁻; KZVO = K₂Zn₂V₁₀O₂₈; DEC = diethyl carbonate; EC = ethylene carbonate; DMIC = dimethyl carbonate; FEC = ethyl methyl carbonate; PDDA-TGO = poly(diallyldimethylammonium chloride) modified reduced graphene oxide; G = propylene carbonate; VGCF = vapor-grown Carbon Fiber; SWNT = single-wall carbon nanotube; MPTA = mesoporous phosphotungstic acid; PDDA-TGO = poly(diallyldimethylammonium chloride) modified reduced graphene oxide.

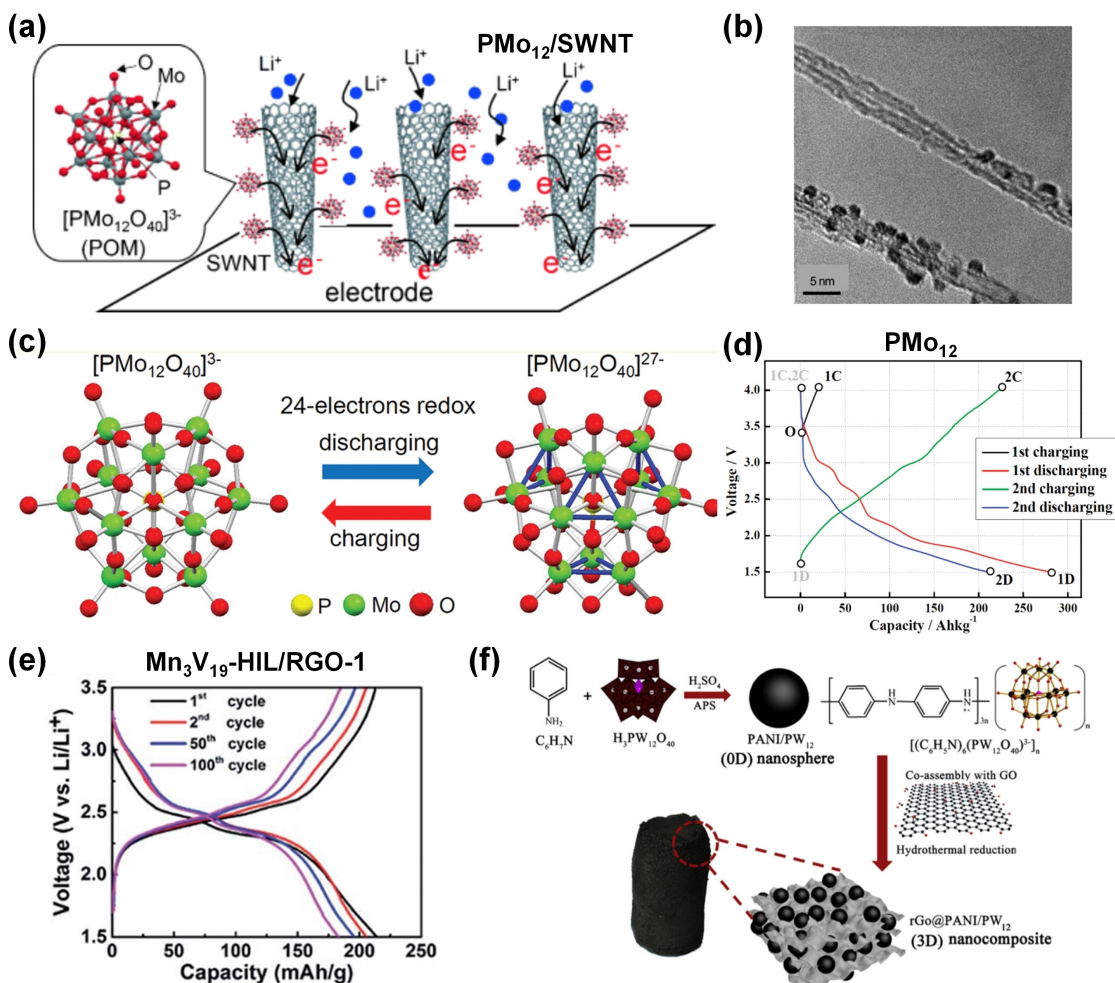


Figure 4. a) Schematic diagram of the expected electrode reaction on the PMo₁₂/SWNT electrode. Reproduced with permission from Ref. [14]. Copyright (2011) Wiley-VCH. b) TEM image of PMo₁₂/SWNT material. Reproduced with permission from Ref. [14]. Copyright (2011) Wiley-VCH. c) Reversible electron process of Keggin-type [PMo₁₂O₄₀]³⁻. Reproduced with permission from Ref. [15]. Copyright (2012) American Chemical Society. d) Charge and discharge curves for the first two cycles of PMo₁₂ electrode. Reproduced with permission from Ref. [15]. Copyright (2012) American Chemical Society. e) Charge/discharge curves of Mn₃V₁₉-HIL/RGO-1 at 100 mA g⁻¹. Reproduced with permission from Ref. [16]. Copyright (2013) Royal Society of Chemistry. f) Schematic diagram of the preparation of 3D rGO@PANI/PW₁₂ cathode. Reproduced with permission from Ref. [17]. Copyright (2017) Elsevier.

abundant active sites to improve the rate performance and cycling stability of the electrode.^[22] Mahajan et al. combined PMo₁₂ encapsulated with polypyrrole (PPy) with a MXene material, Ti₃C₂T_x, to obtain a PMo₁₂@PPy/Ti₃C₂T_x material with a 2D/3D composite structure.^[23] The three components showed synergistic effect in the composite electrode, which simultaneously exhibited high capacity, high cycling stability and superior rate performance. For the PMo₁₂@PPy/Ti₃C₂T_x anode, the main source of the capacity is the reversible multielectron redox of PMo₁₂, while the matrix, Ti₃C₂T_x, provides sufficient active sites and the PPy increases the conductivity of anode and prevents the loss of PMo₁₂.

Although the structures of POMs are mainly determined by the anions, the composition of cation can also significantly affect the electrochemical performance of corresponding POM-electrodes. Lu et al. compared the electrochemical performance of two electrodes containing K₄Na₂V₁₀O₂₈·nH₂O (KNaV₁₀) and Mg₂(NH₄)₂V₁₀O₂₈·nH₂O (MgV₁₀) respectively.^[24] The performance of MgV₁₀-electrode is much better than the performance of

KNaV₁₀-electrode because the one-dimensional Li⁺ tunnels along the *a*-axis direction are formed in MgV₁₀ due to the existence of Mg²⁺, enhancing the kinetics of Li⁺ transportation. This finding can act as a reference for the design of POM structures.

The metal-organic frameworks (MOFs) and POMs are close in size. It is a feasible strategy to combine the POMs and MOF in order to exert their synergistic effect. Wei et al. first applied the combinations of POMs and MOFs into the anode of LIBs. They combined H₅PMo₁₀V₂O₄₀(PMo₁₀V₂) with HKUST-1, a kind of MOF, into combinations named POMOFs, and compounded POMOFs with rGO to obtain POMOFs/rGO (see in Figure 5c).^[25] The rGO ensures satisfactory electrical conductivity, meanwhile, the MOFs buffers the volume change of POMs. Hence, the POMOFs/rGO material exhibits superior cycling stability (see in Figure 5d). Zhao et al. applied another MOF, MIL-88 A, to compound with PMo₁₂. MIL-88 A provides abundant reactive active sites for reversible redox reactions and ion exchange on PMo₁₂, which is conducive to the synergistic effect of the two

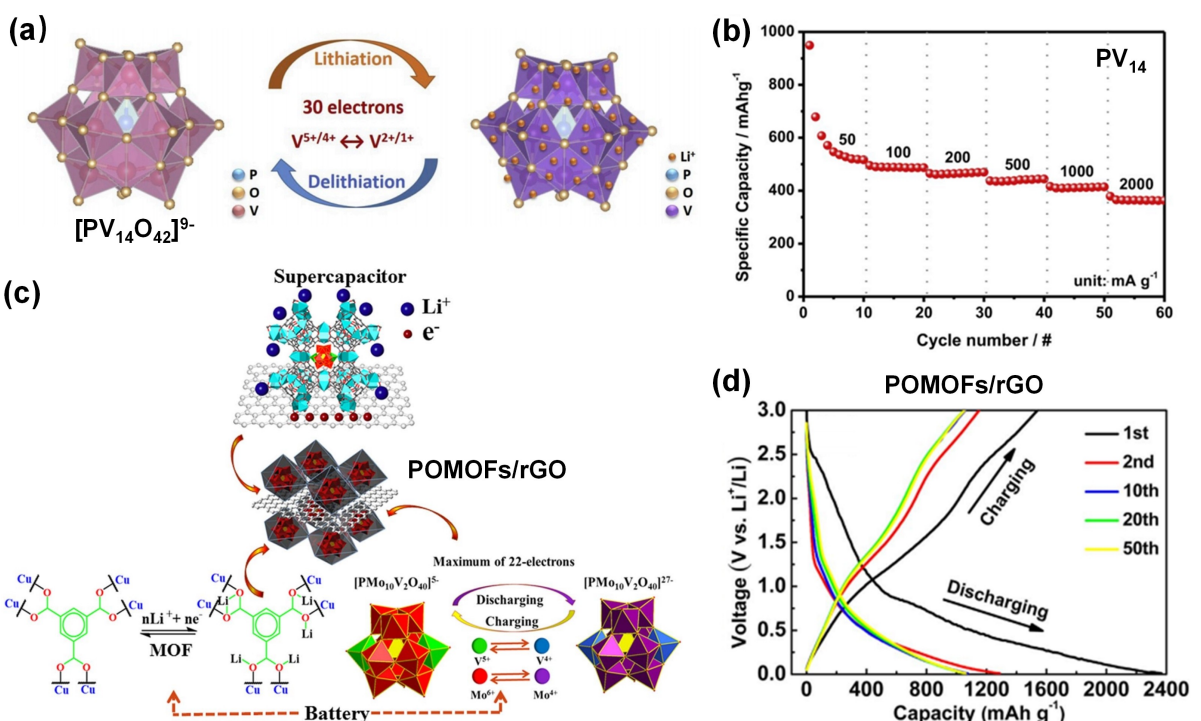


Figure 5. a) Structural schematic diagram of the reversible electron/ion processes of $[PV_{14}O_{42}]^{9-}$. Reproduced with permission from Ref. [18]. Copyright (2019) Elsevier. b) Rate performance of $\text{Na}_0.2\text{H}_2[\text{PV}_{14}\text{O}_{42}] \cdot 7\text{H}_2\text{O}$. Reproduced with permission from Ref. [18]. Copyright (2019) Elsevier. c) Structural schematic diagram of the POMOFs/rGO composite. Reproduced with permission from Ref. [25]. Copyright (2017) Elsevier. d) Charge/discharge curves of a POMOFs/rGO composite sample for five different cycles at a constant current of 50 mA g^{-1} . Reproduced with permission from Ref. [25]. Copyright (2017) Elsevier.

materials thus enhance the ion storage capacity of POMs and the electrochemical performance of electrode.^[26] Jia et al. compounded PMo_{12} with another MOF, a kind of zeolitic imidazolate framework named ZIF-8. The 3D nanomaterial prepared with ZIF-8 and PMo_{12} shows superior reversible specific capacity and cyclic stability when applied to the anode of LIBs.^[27] Apparently, the approach of combining POMs and MOFs can be extended to other kinds of POMs and frameworks with specific properties.

Figures 4(d and e), 5(b and d) show the electrochemical performance of several different POMs. In the delithiated state, the POM-electrode shows a high electrode potential. With the increase of lithium content, the potential of POM-electrode continuously decreases, showing characteristics of solid-solution process. In order to understand the unique characteristics of POMs, it is necessary to compare the POMs with some typical anode/cathode materials.

LiTiO_3 (LTO) and graphite are two typical anode materials. The voltage curve of LTO anode including a voltage plateau exhibits characteristics of phase-separation reaction.^[34] The voltage curve of graphite, which includes several stages corresponding to various intercalation compounds (LiC_6 , LiC_{12} , LiC_{18} , and LiC_{24}), exhibited some characteristics of solid-solution reaction, especially in the early stage of lithium embedding into graphite.^[35] The voltage curve of POM-electrode is similar in shape to the curve of graphite anode, but the voltage curves of POM-anodes are much steeper than that of graphite. Compared with graphite, the average voltage of POMs is higher during charging and discharging. Hence, POM-anodes may not

encounter serious lithium dendrite problems during high-rate charging. $\text{Li}[\text{Ni}_x\text{Co}_y\text{Mn}_z]\text{O}_2$ (NCM),^[36] LiCoO_2 (LCO),^[37] and LFP^[38] are three typical cathode materials. Similarly, the voltage curves of POM-cathodes are much steeper than the voltage curves of NCM, LCO, and LFP. Therefore, for a full battery assembled with POMs as the electrode material, the rate of battery voltage decay may be very high during charging/discharging.

The voltage curves of different POMs are closely related to their own properties, especially the atomic valence change and the structure evolution of POMs with the insertion and extraction of lithium ions. If the average voltage of a kind of POM is relatively low, the LIB using the POM as anode material will have a higher discharge voltage and energy density than the LIB using the POM as cathode material, and thus the POM will be more suitable for anode application. In contrast, if the average voltage of a POM is relatively high, the POM will be more suitable as a cathode material. Horn et al. summarized the previous studies on the POMs applied to the cathode/anode materials of LIBs and their performance including the initial discharge capacity and capacity retention, providing reference for the application and further research of POMs.^[1a]

3.2. Application of POMs in electrode materials for LSBs

LSB is an attractive energy storage system with advantages including low cost, high specific energy, and environmental friendliness.^[39] The application of LSBs still faces many difficulties and challenges. To improve the energy density of

LSBs, it is necessary to increase the sulfur loading.^[39b] However, high-loading sulfur exposed in electrolyte will aggravate the shuttle effect of polysulfide, thus worsening the performance of the batteries.^[39a] In the electrolyte of LSBs, lithium exists in the form of lithium polysulfide, rather than lithium ions that can be reversibly inserted/removed from POMs. Therefore, the ionic sponge characteristics of POMs cannot improve the performance of LSBs. Comparatively, it is the catalytic and adsorption properties of POMs that can accelerate the conversion of polysulfide and improve the efficiency of sulfur loaded the cathode of LSBs. Ye et al. applied Ag(I)-substituted $K_3[H_3Ag^I PW_{11}O_{39}]$ ($Ag^I PW_{11}O_{39}$), a Keggin-type POM with bifunctional catalytic properties, in LSBs.^[10] The dual function of $Ag^I PW_{11}O_{39}$ is related to the presence of both Lewis acidic and basic sites. In $Ag^I PW_{11}O_{39}$, Ag^I ions act as Lewis acidic sites enhancing the adsorption of S, while the external terminal O atoms act as Lewis basic sites interacting with Li atoms of Li_2S_n , hence Li_2S_n can be strongly adsorbed on $Ag^I PW_{11}O_{39}$ (As shown in Figure 6a). Compared with $PW_{12}O_{40}$, $Ag^I PW_{11}O_{39}$ enables LSBs to have more satisfactory cycling stability under the condition of relatively high content and high areal mass loading of active S (see in Figure 6b). Lei et al. composited $[Co_4(PW_9O_{34})_2]^{10-}$ (Co_4W_{18}) with rGO and applied the bifunctional composite electrocatalyst in cathode materials of LSBs.^[40] Figure 6(c) schematically describes the bifunctional catalytic effect of Co_4W_{18} /rGO. The unsaturated Co sites exposed from Co_4W_{18} not only enhance the adsorption of polysulfide, but also reduce the activation energy of polysulfide conversion, thus improving the rate performance and cycling stability of the cathode (see in Figure 6d).

3.3. Application of POMs in electrode materials for SIBs and ZIBs

SIBs and ZIBs, both of which belong to the rocking-chair batteries, work in a similar way to LIBs. Compared with LIBs, the raw materials of SIBs/ZIBs are cheaper and more abundant, making SIBs/ZIBs more cost competitive.^[41] Therefore, SIBs/ZIBs are promising for applications without strict limitations on the volume or mass of the batteries, especially for large-scale electrochemical energy storage and low-speed electric vehicle batteries. Unfortunately, SIBs and ZIBs face similar problems with LIBs, such as the formation of metal dendrites and the resulting safety issues. Some recent studies have attempted to utilize POMs to solve problems in SIBs and ZIBs (Table 1).

Na^+ and Li^+ are both monovalent ions, hence the mechanism of reversible electron reaction of Na^+ in POMs is quite similar to that of Li^+ in POMs. Hartung et al. synthesized rod-like $Na_6[V_{10}O_{28}] \cdot 16H_2O$ by means of the self-assembly of POMs and mixed it with acetylene black into anode material for SIBs.^[30] During charging and discharging, the insertion and extraction of Na^+ in $[V_{10}O_{28}]^{6-}$ is highly reversible, which greatly reduces the irreversible capacity loss and improves the cycling stability of the electrode material. Lin et al. used NPV as the anode material for SIBs and investigated the mechanism of Na^+ storage in NPV.^[29] During the charging and discharging processes, the valence state of V atoms varies between +5 and +3, accompanied by the insertion/extraction of Na^+ between the polyanions and the adsorption/desorption on the surface of NPVs. Shen et al. applied Mn_3V_{19} -HIL/rGO-1 can be used not only as the cathode of LIBs, but also as the cathode of SIBs.^[16] The Mn_3V_{19} -HIL/rGO-1 cathode also shows superior cycling stability (see in Figure 7a) and rate performance in the SIB

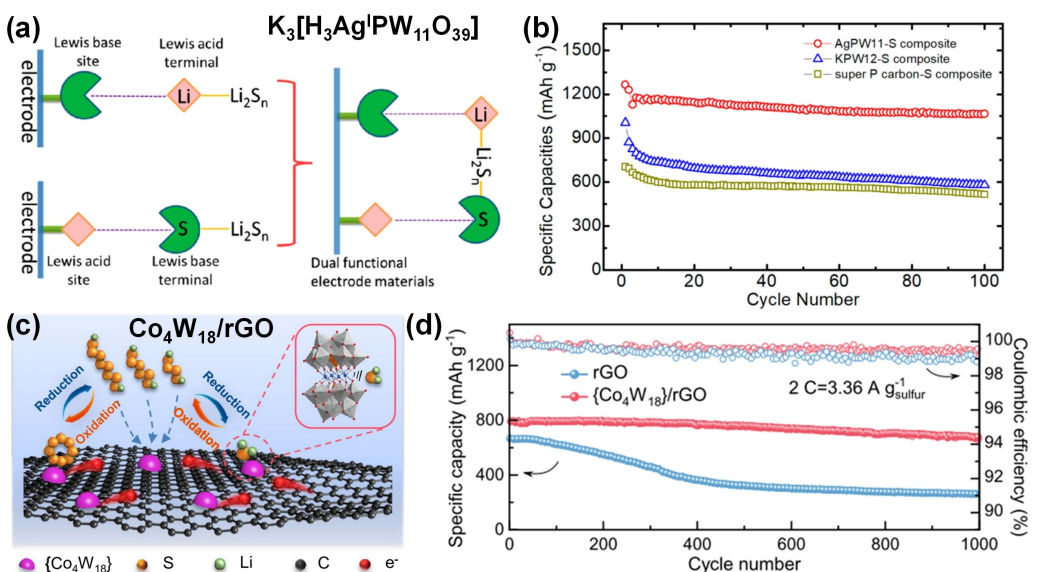


Figure 6. a) Schematic diagram of the bifunctional Ag^I -substituted Keggin $K_3[H_3Ag^I PW_{11}O_{39}]$ regulating the absorbance of Li_2S_n . Reproduced with permission from Ref. [10]. Copyright (2018) American Chemical Society. b) Cycling test of $Ag^I PW_{11}O_{39}/S$ ($Ag^I PW_{11}O_{39}/S$), $PW_{12}O_{40}/S$ (KPW_{12}/S) and super P carbon/S for Li–S battery. Cycling rate: 1 C (1 C = $1.68 A g^{-1}$). Active S mass loading: $1.5 mg cm^{-2}$. Reproduced with permission from Ref. [10]. Copyright (2018) American Chemical Society. c) Schematic diagram of Co_4W_{18} /rGO bifunctionally catalyzing the deposition and oxidation of Li_2S . d) Long-term cycling stability of Co_4W_{18} /rGO composite at 2 C. Reproduced from Ref. [40] under terms of the CC-BY license. Copyright (2022) The Author(s), Published by Springer Nature.

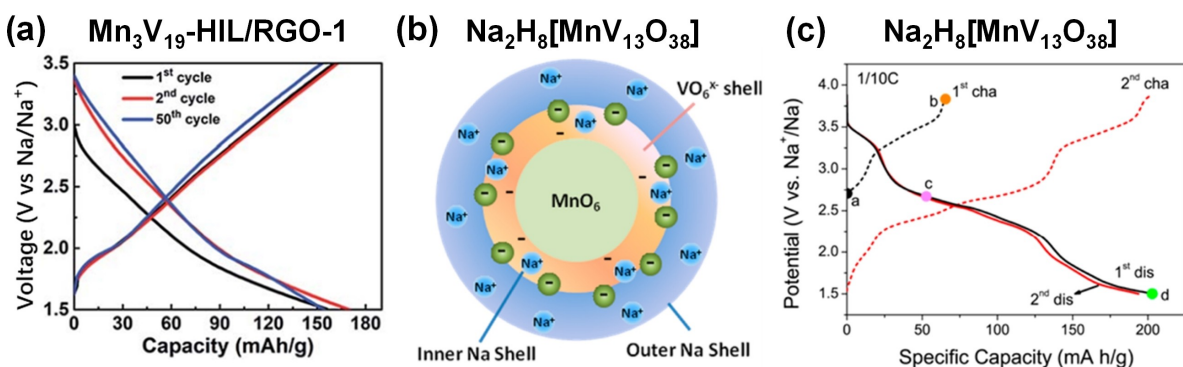


Figure 7. a) The 1st, 2nd, and 50th charge/discharge cycles of Mn_3V_{19} -HIL/RGO-1 as the cathode of SIB in a half cell at 100 mA g^{-1} . Reproduced with permission from Ref. [16]. Copyright (2013) Royal Society of Chemistry. b) Schematic diagram of $\text{Na}_2\text{H}_8[\text{MnV}_{13}\text{O}_{38}]$ as a Na^+ ion sponge and an electron sponge. Reproduced with permission from Ref. [28] Copyright (2017) American Chemical Society. c) Galvanostatic charge/discharge curves of NMV/G cathode cycled at a rate of C/10. Reproduced with permission from Ref. [28]. Copyright (2017) American Chemical Society.

system. The shape of the voltage curve of a POM-electrode is related to the element composition and structure of the POMs, as well as the ions that transfer charge. By comparing Figure 7(a) and Figure 4(e), it is apparently that the voltage curves of a POM used to absorb/release Na^+ and Li^+ can be significantly different. Liu et al. combined $\text{Na}_2\text{H}_8[\text{MnV}_{13}\text{O}_{38}]$ (NMV) and graphene into a cathode material of SIB with acetylene black as the conductive additive in cathode.^[28] Figure 7(b) shows a schematic diagram of NMV acting as an ion/electron sponge. During the battery reaction, each NMV molecule can support the transfer of 11 electrons/ Na^+ -ions, which ensures a high capacity of the cathode (see in Figure 7c). In addition, the molecular structure of NMV is characterized by a 2D flexible network and 1D ion transfer channels, which greatly facilitates the migration of Na^+ . According to the calculation results, the volume change of NMV during charging/discharging is only approximately 7.5%. The above properties make the NMV-modified cathode exhibit good rate performance and cycling stability.

In ZIBs, the charge-transfer ion is Zn^{2+} , which carries twice as much charge as Li^+ . Yang et al. first investigated the Zn^{2+} storage behavior of the $\text{K}_{10}[\text{V}^{IV}_{16}\text{V}^{VI}_{18}\text{O}_{82}]$ (KVO) cluster with mixed valence vanadium element and applied it to the cathode material for ZIBs.^[31] Zhou et al. investigated the performance of $\text{K}_2\text{Zn}_2\text{V}_{10}\text{O}_{28}$ (KZVO) cathode applied for ZIBs.^[32] $\text{Na}_6[\text{V}_{10}\text{O}_{28}]$ can be used as electrode material not only for SIBs as mentioned above, but also for ZIBs. Zhou et al. applied $\text{Na}_6[\text{V}_{10}\text{O}_{28}]$ to the cathode of aqueous ZIBs.^[33] In aqueous ZIBs, the Zn^{2+} diffusion coefficient of $\text{Na}_6[\text{V}_{10}\text{O}_{28}]$ can reach $10^{-10} \text{ cm}^2 \text{s}^{-1}$. The hierarchical structure and electron/ion-sponge properties of KVO, KZVO, and $\text{Na}_6[\text{V}_{10}\text{O}_{28}]$ are beneficial to the migration and intercalation/deintercalation of Zn^{2+} , thus, the zinc ion electrode exhibits high reversible capacity, remarkable rate performance and excellent cycling stability.

4. Conclusions and Perspectives

In the research of electrode materials, POMs are promising active materials. Suitable POMs introduced into battery electro-

des can not only improve the capacity and power density of the electrodes, but also improve the rate performance, cycling stability and service life due to the ion/electron-sponge properties, hierarchical structures, flexible frameworks, high reversible reactivity, and diverse application strategies of POMs. For a POM-electrode where POMs act as ion/electron sponges, during the charging/discharging processes, the valence state of the transition metal atoms are constantly changing, accompanied by the transfer of electrons between electrodes, the insertion/extraction of ions (such as Li^+ and Na^+) between the polyanions, and the adsorption/desorption of ions on the surface of POMs. These POMs can be used as the cathode and anode materials, even the same POM. This is because the electrode potential of a POM-electrode is generally lower than the electrode potential of commonly used cathodes (NCM, LCO, LFP, etc.) and higher than the electrode potential of typical anodes (graphite, lithium metal, etc.). In addition to being used as ion/electron sponges, POMs with active sites can catalyze the conversion of battery reaction intermediates, especially the conversion of lithium polysulfides in LSBs. As a result, POMs have broad prospects in the applications of electrode materials and electrochemical energy storage.

However, the practical application of POMs in electrode materials is still challenging. According to the equation $\text{Energy} = \text{Capacity} \times \text{Voltage}$, the capacity and charge/discharge voltage are both important factors determining the energy density of electrodes. As shown in Figures 4 and 5, when the POMs act as the active material in electrodes and deliver satisfactory capacity, the voltage curves are not ideal enough. There is no obvious plateau in the voltage curves. Compared with the voltage curves of commonly used electrode materials such as NCM,^[36] LCO,^[37] and LFP,^[38] the voltage curves of POMs are much steeper. For a full battery assembled with POMs as the electrode material, the rate of battery voltage decay may be very high during discharge. Therefore, the biggest challenge of applying POMs as electrode materials comes from their voltage characteristics.

In order to further improve the performance of POMs to meet the requirements as electrode materials, it is practicable

to modify the intrinsic structure of the POMs and the structural design of the POM-electrodes:

- (1) Modify the anions of the POMs. The central atoms of the anions affect many properties of the POMs, including the change of valence state, the number of transferred electrons, and the charging/discharging curves when POMs are applied in electrodes to store/release ions such as Li^+ , Na^+ , and Zn^{2+} . The average voltage of POM-cathode or POM-anode can be increased or decreased by using appropriate anions, thus enabling the POM-battery to have a high energy density. In LSBs, the catalytic performance of POMs is more important than the ion-storage property. By doping the anions of the POMs with other metallic cations, the charge distribution in the POMs can be adjusted, thus the interaction between the abundant terminal O atoms and Li_2S_n can be regulated (such as $\text{Ag}^+\text{PW}_{11}\text{O}_{39}$ ^[10]). Therefore, the electrode performance can be enhanced by adjusting the central atom of the anions with suitable atoms especially transition metal atoms.
- (2) Modify the cations of the POMs. As mentioned above, the voltage curves of POMs are various when the POMs absorb/release different cations due to the size effect of the cations. The change of cations in POMs will directly regulate the ion channels in POMs, thus affect the thermodynamics and dynamics of ion transfer and eventually adjust the electrochemical performance of the POMs.
- (3) Modify the structural design of the composite materials in POM-electrodes. In previous studies, the combination of POMs with materials such as SWNTs, rGO, and MOFs has been shown to improve the conductivity of the electrode or increase the number of active sites for electrode reactions, thus facilitating electron transport and ion reactions. As for POM-electrodes, the type and structure of materials outside the POMs have a considerable impact on the performance of POMs as well. Suitable material and well-designed structure will facilitate the synergistic effect between POMs and other components, ultimately enhancing the performance of the POM-electrodes.

At present, the POM-electrodes applied in LIBs have attracted more attention than the POM-electrodes applied in other battery systems. Only a few studies have been conducted on electrode modification of LSBs using POMs. For SIBs and ZIBs, which work in a similar mechanism with LIBs but have a lower cost than LIBs, the research of POMs as electrode materials is still in its infancy. Although many previous studies have reported the remarkable performance of POMs when applied in electrode materials, the fundamental science of POMs still needs more in-depth exploration, including the charge carrier behaviors, mechanism of self-assembly behaviors, relationship between charge/discharge voltage curves and the structures of POMs, ion storage behaviors and related structure evolution during ionic reactions.^[5a] In addition to further research on the mechanisms and fundamentals, the optimization of electrode preparation strategy is also beneficial to improve the performance of POM-electrodes.^[42]

Acknowledgements

We would like to show gratitude to the National Natural Science Foundation of China (No. 22279070 [L.W.], and U21A20170 [X.H.]) and the Ministry of Science and Technology of China (No. 2019YFA0705703 [L.W.]). We want to thank the "Explorer 100" cluster system of Tsinghua National Laboratory for Information Science and Technology for their facility support.

Conflict of Interest

The authors declare no conflict of interest.

Data Availability Statement

The data that support the findings of this study are available from the corresponding author upon reasonable request.

Keywords: electrochemical performance • electrode modification strategies materials • polyoxometalates • secondary batteries

- [1] a) M. R. Horn, A. Singh, S. Alomari, S. Goberna-Ferrón, R. Benages-Vilau, N. Chodankar, N. Motta, K. Ostrikov, J. MacLeod, P. Sonar, P. Gomez-Romero, D. Dubal, *Energy Environ. Sci.* **2021**, *14*, 1652–1700; b) N. Casañ-Pastor, P. Gómez-Romero, *Front. Biosci.* **2004**, *9*, 1759–1770; c) B. Huang, D.-H. Yang, B.-H. Han, *J. Mater. Chem. A* **2020**, *8*, 4593–4628.
- [2] J. J. Berzelius, *Ann. Phys.* **1826**, *82*, 369–392.
- [3] P. Gómez-Romero, M. Lira-Cantú, *Adv. Mater.* **1997**, *9*, 144–147.
- [4] a) J. Deng, C. Bae, A. Denlinger, T. Miller, *Joule* **2020**, *4*, 511–515; b) A. Masias, J. Marcicki, W. A. Paxton, *ACS Energy Lett.* **2021**, *6*, 621–630.
- [5] a) L. Yang, J. Lei, J.-M. Fan, R.-M. Yuan, M.-S. Zheng, J.-J. Chen, Q.-F. Dong, *Adv. Mater.* **2021**, *33*, 2005019; b) J. Wang, Y. Liu, Q. Sha, D. Cao, H. Hu, T. Shen, L. He, Y.-F. Song, *ACS Appl. Mater. Interfaces* **2022**, *14*, 1169–1176; c) N. I. Gumerova, A. Rompel, *Nat. Chem. Rev.* **2018**, *2*, 0112.
- [6] G.-M. Bosch, A. Sarapulova, S. Dsoke, *ChemElectroChem* **2021**, *8*, 656–664.
- [7] L. Ni, G. Yang, Y. Liu, Z. Wu, Z. Ma, C. Shen, Z. Lv, Q. Wang, X. Gong, J. Xie, G. Diao, Y. Wei, *ACS Nano* **2021**, *15*, 12222–12236.
- [8] J. J. Carbó, C. Bo, J. M. Poblet, in *Comprehensive Inorganic Chemistry II (Second Edition)*, (Eds: J. Reedijk, K. Poepelmeier), Elsevier, Amsterdam 2013.
- [9] D.-L. Long, R. Tsunashima, L. Cronin, *Angew. Chem. Int. Ed.* **2010**, *49*, 1736–1758; *Angew. Chem.* **2010**, *122*, 1780–1803.
- [10] J. C. Ye, J. J. Chen, R. M. Yuan, D. R. Deng, M. S. Zheng, L. Cronin, Q. F. Dong, *J. Am. Chem. Soc.* **2018**, *140*, 3134–3138.
- [11] T. Ueda, *ChemElectroChem* **2018**, *5*, 823–838.
- [12] J. Gu, W. Chen, G. G. Shan, G. Li, C. Sun, X. L. Wang, Z. Su, *Mater. Today* **2021**, *21*, 100760.
- [13] H. Yoshikawa, C. Kazama, K. Awaga, M. Satoh, J. Wada, *Chem. Commun.* **2007**, 3169–3170.
- [14] N. Kawasaki, H. Wang, R. Nakanishi, S. Hamanaka, R. Kitaura, H. Shinohara, T. Yokoyama, H. Yoshikawa, K. Awaga, *Angew. Chem. Int. Ed.* **2011**, *50*, 3471–3474; *Angew. Chem.* **2011**, *123*, 3533–3536.
- [15] H. Wang, S. Hamanaka, Y. Nishimoto, S. Irle, T. Yokoyama, H. Yoshikawa, K. Awaga, *J. Am. Chem. Soc.* **2012**, *134*, 4918–4924.
- [16] F.-C. Shen, Y.-R. Wang, S.-L. Li, J. Liu, L.-Z. Dong, T. Wei, Y.-C. Cui, X. L. Wu, Y. Xu, Y.-Q. Lan, *J. Mater. Chem. A* **2018**, *6*, 1743–1750.
- [17] L. Ni, G. Yang, C. Sun, G. Niu, Z. Wu, C. Chen, X. Gong, C. Zhou, G. Zhao, J. Gu, W. Ji, X. Huo, M. Chen, G. Diao, *Mater. Today* **2017**, *6*, 53–64.
- [18] S.-C. Huang, C.-C. Lin, C.-W. Hu, Y.-F. Liao, T.-Y. Chen, H.-Y. Chen, *J. Power Sources* **2019**, *435*, 226702.

- [19] H. Ilbeygi, I. Y. Kim, M. G. Kim, W. Cha, P. S. M. Kumar, D.-H. Park, A. Vinu, *Angew. Chem. Int. Ed.* **2019**, *58*, 10849–10854; *Angew. Chem.* **2019**, *131*, 10965–10970.
- [20] T.-Y. Chen, H. V. Thang, T.-Y. Yi, S.-C. Huang, C.-C. Lin, Y.-M. Chang, P.-L. Chen, M.-H. Lin, J.-F. Lee, H.-Y. T. Chen, C.-C. Hu, H.-Y. Chen, *ACS Appl. Mater. Interfaces* **2022**, *14*, 52035–52045.
- [21] Y. Ji, J. Hu, L. Huang, W. Chen, C. Streb, Y.-F. Song, *Chem. Eur. J.* **2015**, *21*, 6469–6474.
- [22] Q. Li, M. Xu, T. Wang, H. Wang, J. Sun, J. Sha, *Chem. Eur. J.* **2022**, *28*, e202200207.
- [23] M. Mahajan, G. Singla, S. Ogale, *ACS Appl. Energ. Mater.* **2021**, *4*, 4541–4550.
- [24] S. Lu, Y. Lv, W. Ma, X. Lei, R. Zhang, H. Liu, X. Liu, *Inorg. Chem. Front.* **2017**, *4*, 2012–2016.
- [25] T. Wei, M. Zhang, P. Wu, Y.-J. Tang, S.-L. Li, F.-C. Shen, X.-L. Wang, X.-P. Zhou, Y.-Q. Lan, *Nano Energy* **2017**, *34*, 205–214.
- [26] X. Zhao, G. Niu, H. Yang, J. Ma, M. Sun, M. Xu, W. Xiong, T. Yang, L. Chen, C. Wang, *CrystEngComm* **2020**, *22*, 3588–3597.
- [27] X. Jia, J. Wang, H. Hu, Y.-F. Song, *Chem. Eur. J.* **2020**, *26*, 5257–5263.
- [28] J. Liu, Z. Chen, S. Chen, B. Zhang, J. Wang, H. Wang, B. Tian, M. Chen, X. Fan, Y. Huang, T. C. Sum, J. Lin, Z. X. Shen, *ACS Nano* **2017**, *11*, 6911–6920.
- [29] C.-C. Lin, W.-H. Lin, S.-C. Huang, C.-W. Hu, T.-Y. Chen, C.-T. Hsu, H. Yang, A. Haider, Z. Lin, U. Kortz, U. Stimming, H.-Y. Chen, *Adv. Mater. Interfaces* **2018**, *5*, 1800491.
- [30] S. Hartung, N. Bucher, H.-Y. Chen, R. Al-Oweini, S. Sreejith, P. Borah, Z. Yanli, U. Kortz, U. Stimming, H. E. Hostler, M. Srinivasan, *J. Power Sources* **2015**, *288*, 270–277.
- [31] K. Yang, Y. Hu, L. Li, L. Cui, L. He, S. Wang, J. Zhao, Y.-F. Song, *Nano Energy* **2020**, *74*, 104851.
- [32] T. Zhou, L. Zhu, L. Xie, Q. Han, X. Yang, X. Cao, J. Ma, *Small* **2022**, *18*, 2107102.
- [33] T. Zhou, L. Xie, Q. Han, X. Yang, L. Zhu, X. Cao, *Chem. Eng. J.* **2022**, *445*, 136789.
- [34] G.-N. Zhu, Y.-J. Du, Y.-G. Wang, A.-S. Yu, Y.-Y. Xia, *J. Electroanal. Chem.* **2013**, *688*, 86–92.
- [35] a) Q. Liu, S. Li, S. Wang, X. Zhang, S. Zhou, Y. Bai, J. Zheng, X. Lu, *J. Phys. Chem. Lett.* **2018**, *9*, 5567–5573; b) S. Zhang, M. S. Ding, K. Xu, J. Allen, T. R. Jow, *Electrochim. Solid-State Lett.* **2001**, *4*, A206.
- [36] H.-J. Noh, S. Youn, C. S. Yoon, Y.-K. Sun, *J. Power Sources* **2013**, *233*, 121–130.
- [37] K. Wang, J. Wan, Y. Xiang, J. Zhu, Q. Leng, M. Wang, L. Xu, Y. Yang, *J. Power Sources* **2020**, *460*, 228062.
- [38] A. S. Andersson, J. O. Thomas, B. Kalska, L. Häggström, *Electrochim. Solid-State Lett.* **2000**, *3*, 66.
- [39] a) H.-J. Peng, J.-Q. Huang, X.-B. Cheng, Q. Zhang, *Adv. Energy Mater.* **2017**, *7*, 1700260; b) A. Bhargav, J. He, A. Gupta, A. Manthiram, *Joule* **2020**, *4*, 285–291.
- [40] J. Lei, X.-X. Fan, T. Liu, P. Xu, Q. Hou, K. Li, R.-M. Yuan, M.-S. Zheng, Q.-F. Dong, J.-J. Chen, *Nat. Commun.* **2022**, *13*, 202.
- [41] J.-Y. Hwang, S.-T. Myung, Y.-K. Sun, *Chem. Soc. Rev.* **2017**, *46*, 3529–3614.
- [42] J. Hu, Y. Ji, W. Chen, C. Streb, Y.-F. Song, *Energy Environ. Sci.* **2016**, *9*, 1095–1101.

Manuscript received: December 6, 2022

Revised manuscript received: February 16, 2023

Accepted manuscript online: February 16, 2023

Version of record online: March 8, 2023